

© Performance Analysis of an Improved 3D PET Monte Carlo Simulation and Scatter Correction

C.H. Holdsworth, *Student Member, IEEE*, C.S. Levin*, *Member, IEEE*, M. Janecek, *Student Member, IEEE*, M. Dahlbom, *Senior Member, IEEE*, E.J. Hoffman, *Fellow, IEEE*
UCLA School of Medicine, UCSD School of Medicine* and San Diego VA Medical Center*

Abstract

We are developing an accelerated Monte Carlo simulation of PET that can be used for scatter correction of 3D PET data. Our Monte Carlo technique accurately accounts for single, multiple, and dual Compton scatter events, attenuation through the patient bed, activity from outside the field of view, and the true energy response of the scanner. We have incorporated innovative sampling techniques that are compatible with our simulation approach, increasing efficiency by a factor of seven. We have reduced the error in the resulting total output distributions to $<1\%$. The execution time to acquire 10 million scatter coincidence events for a 3D thorax PET scan is only 4 minutes on a 300MHz Sun dual processor workstation. We demonstrate that when low noise input data is used, images corrected using the Monte Carlo 3D PET scatter correction demonstrate no statistically significant deviation from true activity concentration when accurate input data was used. The speed and accuracy of our simulation program makes it a powerful research tool and a practical scatter correction for 3D PET clinical imaging.

I. INTRODUCTION

Detected scatter events degrade image contrast and compromise quantitative accuracy in PET. Scatter effects become a significant problem especially in 3D PET when the lead septa are removed to achieve a 5-fold increase in sensitivity. The scatter fraction for whole body 3D PET studies increases from 10-20% in 2D PET to 40-60% in 3D PET [1]. Scatter correction for the resulting images is a challenging problem. Analytical calculation and correction of the scatter distribution acquired from a PET scan is difficult, particularly when calculating multiple or dual scatter [2].

Monte Carlo computer simulations use the known initial conditions and physics of a system to generate data using random numbers to determine probabilistic behavior. The accuracy of the simulated data is limited only by the accuracy of the input data and the detail of the model employed in the simulation. This technique can solve complex problems that are impossible to solve analytically.

Although techniques have been used to reduce computation times in other Monte Carlo Simulations for PET [3,4,5,6], these programs are not designed primarily for speed. Typical execution rates of a simulated 3D PET thorax acquisition are on the order of 2-5 ms per acquired event on a 300MHz Sun dual processor workstation [7,8]. At this acquisition rate, it

takes over a day to simulate the equivalent of 10 million equally weighted scatter coincidence events.

Our accelerated Monte Carlo code simulates 10 million detected scatter coincidence events in only 4 minutes on a 300MHz Sun dual processor workstation. The short execution time makes this simulation an effective tool for detailed investigation of the effect of scatter in PET imaging. The accelerated Monte Carlo simulation is now fast enough for scatter correction of clinical 3D PET studies.

The Monte Carlo method of 3D PET scatter correction is activity distribution and attenuation media dependent. To perform a Monte Carlo calculated scatter correction for a 3D PET scan, the emission image volume is first reconstructed to generate the relative activity distribution that determines the number of annihilations to simulate in each voxel. The transmission data is reconstructed to create the voxelized attenuation map that helps determine the interactions of individual simulated photons. The Monte Carlo code uses these data to generate a scatter distribution that can be scaled and then subtracted from the original normalized sinogram prior to a second image reconstruction. The Monte Carlo scatter correction has the potential for greater accuracy than any other method currently employed [3].

II. MATERIALS AND METHODS

A. Simulation

Our simulation code was originally written in C-Language [9,10]. We streamlined the program, implemented some simple variance reduction techniques, and improved the efficiency by a factor of 24 while improving the accuracy of the program [11]. For this paper, we employed innovative variance reduction techniques and improved the efficiency of the program by an additional factor of seven while further reducing the error to $<1\%$. Simulations were performed on a dual 300MHz processor Sun Ultra II Creator workstation. Although the data presented in this paper is the result of simulations of the Siemens/CTI ECAT EXACT HR+ 962 PET system, our Monte Carlo code can simulate any ring geometry.

For evaluation of the simulation and scatter correction accuracy, we used emission and transmission data with a large number of events to minimize noise effects. We currently use the system's simulation-based scatter correction [12] during reconstruction of the emission image volume to provide a

more accurate initial activity distribution. Once the required data is read into memory, the relative number of annihilations to be simulated in each voxel is determined by the emission image. Annihilations are not simulated in air voxels.

The transmission image determines the attenuation coefficient in each voxel. We have found that the simulation is sensitive to inaccuracy in the voxelized attenuation map. Median smoothing and thresholding is used to reduce the effects of noise while retaining adequate resolution for edge detection. Annihilation photons are transported through the medium using the very efficient Delta Scattering method [13] that is accurate to within 0.07% [11]. The simulated photons are propagated through the attenuation map using random numbers to determine locations and results of interactions. If a Compton scatter event occurs, the new direction and energy of the scattered photon is determined using tabulated values derived from a product of the actual energy response of the scanner [14] and data generated by the Klein-Nishina formula (see section III.B). Once a photon escapes the body, it is transported to the detector gantry. If both photons from an annihilation are detected, a coincidence event is recorded. The event is considered 'scatter' if either of the detected photons recorded a Compton scatter interaction, and a 'primary' event otherwise. After all annihilations in every voxel of the activity distribution have been simulated, the program writes the scatter and primary sinograms to a file.

To employ a scatter correction, the simulated total distribution (sum of primary and scatter) is scaled to match the original normalized measured sinogram. The properly scaled simulated scatter distribution can then be subtracted from the measured sinogram prior to reconstruction.

B. Phantom

To obtain our original sinogram data, we used a tissue-equivalent anthropomorphic phantom of the thorax (Radiology Support Devices, Inc., Long Beach, CA) containing fillable cavities and organs to closely simulate an actual patient's geometry. All compartments are filled with known activity levels, and there is no activity in the center of the heart chamber, the spine, or the lungs. The phantom was scanned using a Siemens/CTI 962 HR+ PET scanner with septa removed. We acquired a 200 million-count, three bed position emission scan and a 45-minute transmission scan to reduce noise and error in the input images. 2D transmission scan data was processed to generate 3D attenuation correction data.

C. Techniques for Reducing Execution Time

The long execution time of most Monte Carlo 3D PET simulations limits data collection for research applications and makes their use prohibitive for practical image correction. Therefore, most of our effort was spent optimizing the code for fast execution. In this section, we present techniques employed to reduce execution time and increase accuracy.

Our simulation utilizes an accurate photon transport method known as Delta Scattering [13]. Because photons do not have to be 'stepped through' the attenuation medium, this method is fast and independent of matrix size; however, this

technique is not compatible with certain variance reduction techniques such as forced detection and stratification [15].

We have developed a stratification algorithm that is compatible with our method of photon transport. The stratification has two components. To reduce error and to avoid wasting computation time on simulating annihilation photons that are unlikely to result in coincidence detection, we implement an acceptance angle that depends on axial position. The second component is to split the second photon of an annihilation pair into multiple photons of equal weight, when the first photon is detected. The amount of second photon splitting also depends on emission angle and position. Information to optimize these stratification techniques for different objects is obtained during preprocessing (1 minute) prior to simulation. The preprocessing time is included in the total simulation time quoted.

Most PET simulations use a stratification technique in which only photons emitted within an initial axial acceptance angle limit around the PET gantry are simulated. This saves the computation time by not simulating annihilations that are not likely to result in coincidence. By using an acceptance angle limit of 40° rather than 180° in our code, 4.6 times the number of coincidences are acquired for the same execution time with a 4% loss of scatter events. The resulting acquisition rate is 42 detected scatter coincidence events per ms. Using an acceptance angle of 70° the acquisition rate is 35 scatter events per ms with 0.1% loss of scatter events. We now implement an acceptance angle that depends on axial position. The axial acceptance angle can be narrow in the center of FOV, but must wider, especially outside the FOV, to avoid losing a significant number of detectable scatter events. In addition, for some axial positions outside the FOV, there is no need to simulate photons that are emitted within 5° to 10° of the gantry plane. Data for optimal acceptance angles are obtained during preprocessing. Using the optimal acceptance angle, our simulation acquired 44 scatter coincidence events per ms with only a 0.3% loss.

In Monte Carlo methods, a single photon can be divided into multiple photons, provided the resulting photons are weighted such that the sum of their weights is one. This method is known as *photon splitting* and will not bias the results of a simulation. If the first photon of an annihilation pair is detected, we simulate multiple second photons. This is done so most single photon detection events will result in at least one coincidence detection. The degree of second photon splitting depends on axial position and emission angle. Less splitting is used for second photons that are more likely to be detected. Using this method, the number of detected scatter coincidence events is increased by a factor of 3 to 4 depending on phantom geometry.

In order to implement the second photon splitting technique without adding noise to the scatter distribution, it is important to consider two cases. When the first photon is detected without being scattered, the second photon is split at the point of annihilation. If the first photon undergoes a scatter event, we stop it before it scatters, and simulate the second photon. If the second photon is detected, we split the

first photon at the point of scatter. If the second photon is not detected, we begin the next annihilation.

To see if this method of stratification had any effect on simulation results, we ran simulations using the previous version of the code without limiting acceptance angle for a high number of counts. We saw no statistically significant difference between simulation sinograms for a noise level of 2%.

To incorporate the true energy response of the scanner and reduce computation time, we force photons undergoing Compton interactions to stay above the realistic energy cutoff of the system. This is done by storing values incorporating the effect of a product of the Klein-Nishina formula with the energy response of the system into an array. This prevents loss of ~50% of the individual scattered photons in our simulation while maintaining equally weighted scatter coincidence events. In addition, calculation of scatter angle and energy for scattered photons is now replaced by a single memory access. For multiple scatter events, the scattered photons are accepted or rejected depending on their probability of occurrence. When simulating a multiply scattered photon, this probability must take into account that the photon has already been accepted by the system's energy response in earlier scatter interactions. This technique doubled the efficiency of our program and increased its accuracy. The effect of the energy resolution of the system is shown in figure 1.

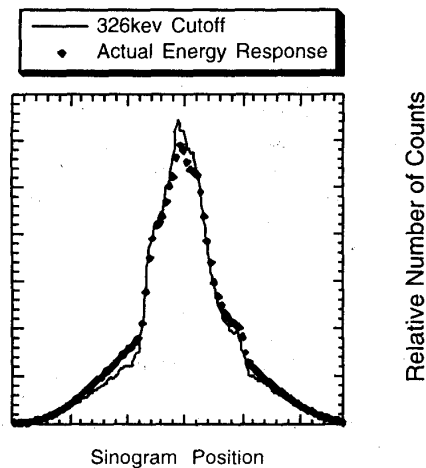


Figure 1. The scatter distribution is broader when the 23% energy resolution of the system is taken into account.

The principle of taking into consideration the energy response of the detectors before photons ever reach the detectors can be applied to other modalities. It would be especially effective in simulating CT or X-ray imaging where a polychromatic beam is used. By scaling the number simulated photons for each energy by the energy response of the system prior to simulation and using our method for Compton scatter interactions, the noise in simulated data could be significantly reduced; however, this technique will corrupt the nature of the noise. For general Monte Carlo simulation,

there is no reason to simulate events in chronological order. As long as probabilities are kept consistent, events can be simulated in the order that results in the best efficiency.

Our code currently acquires 44,000 scatter coincidences per second. This allows us to do multiple simulations per day, and subtle changes in the code can be made and tested quickly, giving rapid feedback on the accuracy of the simulation and the nature of scatter in PET. The reduced computation time is especially necessary if we want to implement the Monte Carlo 3D PET scatter correction in the clinic.

The efficiency of our program demonstrates the potential of a Monte Carlo simulation designed for a specific application. In this case, modeling of the scatter in 3D PET.

III. RESULTS

A. Accuracy

To test the accuracy of the new program, we compared the original measured image before scatter correction to the simulated total image. These images contain both the scatter and primary distributions, and theoretically these images should be identical (see figure 2). The smoother appearance of the simulated image is due to lower noise in simulated data, and a slight loss of resolution due to rebinning of sinogram data into CTI system 7 format prior to filtered back projection.



Figure 2. The left image is reconstructed without scatter correction from measured PET scanner data. The right image is reconstructed from simulated data.

Quantitative analysis of accuracy of the simulated image is given in Table 1. ROI analysis was performed to measure the level of scatter in five different regions in the thorax images.

Table 1. A comparison between the simulated totals image and the original PET image without scatter correction.

Mean ROI Values of Image Intensity		
Location of ROI	Monte Carlo Image of Primary + Scatter	Emission Image with no Scatter Correction
Heart Wall	4.59 ± 0.10	4.60 ± 0.11
Background	1.97 ± 0.03	2.01 ± 0.04
Center of Heart	1.03 ± 0.02	1.04 ± 0.04
Lung	0.24 ± 0.01	0.24 ± 0.02
Backbone	0.65 ± 0.02	1.04 ± 0.03

The error in the backbone region is due to the fact that the attenuation of bone structures was set equivalent to that of tissue in our attenuation map processing. This is not a good approximation and it will have to be corrected in future work. Otherwise, there is no statistically significant error.

B. Multiple Scatter

On the order of 25-30% of the total scatter distribution consists of multiple and dual scatter events [10]. These are especially difficult to calculate analytically. In fact, most scatter corrections ignore these effects [2,12]. In dual scatter events, both detected photons have been scattered. In multiple scatter events, one photon has been scattered more than once. These two different forms of scatter have different distributions and originate from different locations. Dual scatter originates mostly from annihilations at the center of the FOV with contribution falling off towards the edges in a triangle shape. The width of the triangle decreases with increasing emission angle. The resulting distribution is broader and very different from the single scatter distribution. Both of these observations seem to be independent phantom geometry. Multiple scatter events behave more like single scatter events both in original location of contributing annihilations and in the resulting distribution. When these two different types of scatter are isolated, their origination and effect on the scatter distribution are somewhat predictable. This suggests that it may be possible to add the effect of both types of multiple scatter events, to good approximation, to analytical scatter corrections currently based only on single scatter [2,12] using empirical Monte Carlo simulation data.

C. Scatter Correction

To apply the Monte Carlo Scatter Correction to 3D PET studies in the clinic, the emission sinogram must first be reconstructed to obtain the activity distribution. We use the scatter correction method already on the system [12] for a best estimate of the activity distribution. The transmission scan is processed in parallel to obtain the attenuation map (reconstructed in 2-D). The scatter sinogram is then calculated (currently in 4 minutes) using the Monte Carlo simulation. After subtracting the smoothed and scaled scatter estimate from the original normalized sinogram (1 minute), the resulting sinogram can be reconstructed to produce the final image. Thus, the current time cost of employing the Monte Carlo scatter correction is one extra 3D reconstruction, 1 minute of smoothing, and a 4 minute simulation.

We compared the performance of the Monte Carlo 3D PET scatter correction with one of the most accurate analytical scatter corrections currently available [12]. Figure 3 compares images reconstructed using the 3D PET scatter correction currently available on Siemens scanner and the Monte Carlo scatter correction.



Figure 3. The image using the analytical scatter correction is on the left. The right image used the Monte Carlo scatter correction.

ROI values of five different regions in each image were compared with actual activity concentration levels in the phantom. Table 2 contains results of the quantitative analysis.

Table 2. Comparing scatter corrected ROI values with true activity concentrations. Activity values are in $\mu\text{Ci/ml} \cdot 10^{-1}$.

Mean ROI Values of Activity Concentration			
Location of ROI	MC Scatter Correction	CTI's Scatter Correction	Activity in Phantom
Heart Wall	9.2 ± 0.6	9.5 ± 0.6	9.1 ± 0.2
Background	3.80 ± 0.12	4.07 ± 0.10	3.73 ± 0.04
Center of Heart	0.06 ± 0.10	0.64 ± 0.11	0
Lung	0.02 ± 0.08	0.14 ± 0.08	0
Backbone	-0.45 ± 0.06	-0.53 ± 0.06	0

Corrected for Partial Voluming Effects in Respective ROI's.

Concentration values in the ROI's for the heart wall have been corrected for partial volume and resolution effects. We had to be careful to avoid streak artifacts from filtered back projection in ROI's drawn in the lung. In the future, we plan to use iterative reconstruction for better quantitative accuracy. The image using the Monte Carlo scatter correction is more accurate than the scatter correction currently available on Siemens scanners for all regions. There is no statistically significant error in the Monte Carlo scatter corrected image, except in the spine ROI where attenuation data was incorrect.

IV CONCLUSION

Our accelerated Monte Carlo simulation for an ECAT HR+ 3D PET scan currently acquires 2.5 million detected scatter coincidence events per minute. This is ~250 times faster than most other available Monte Carlo PET simulations [3,4,5,6] and ~150 times faster than our original code [9,10]. No statistical inaccuracy was seen for a noise level of 2% in regions where input data was accurate.

We improved the accuracy and efficiency of our program using innovative variance reduction techniques. We have increased the sophistication of the stratification algorithm by having the acceptance angle depend on axial position. In addition, the degree of second photon splitting depends on position and emission angle. We incorporated the detection probability for different photon energies while also increasing computational efficiency. The Monte Carlo scatter correction for 3D PET was more accurate than the scatter correction currently available on Siemens PET scanners when low noise input data was used. The scanner's scatter correction did not incorporate multiple scatter, dual scatter, or scatter from outside the FOV. In the future, we will compare the MC scatter correction to an analytical technique that does incorporate scatter from outside the FOV.

Small animal 3D PET scanners such as MicroPET are being used in research where quantitative analysis is preformed. Although we expect the scatter fraction to be lower because a mouse or rat has less scatter medium than a human being, there is also less attenuation in any scatter

generated. In addition, there is no end shielding, the lower energy threshold is 250keV (compared to 350keV), scattered photons have greater absorption efficiency relative to primary photons in the shorter detector crystals, and there may be significant scatter off of the subject's bed. We want to use Monte Carlo Simulation to analyze scatter in animal scanner imaging and explore the possibility of employing a scatter correction and a Monte Carlo attenuation correction on sinogram data.

We are currently investigating methods of input data processing, particularly techniques to reduce noise in the attenuation map without smoothing edges [16,17,18]. We intend to take a more detailed look at the nature of scatter in PET, including the type of scatter, and the effects of annihilation position, emission angle of photon, scattered photon energy, subject geometry, etc. We also want to continue to study scatter correction performance on phantom distributions with varying noise levels and on patient data for clinical 3D PET thorax studies.

V. ACKNOWLEDGMENTS

The authors would like to thank Dr. Robert Harrison for discussions on variance reduction techniques and Dr. Charles Watson for information on detection response efficiency as a function of energy. The authors would also like to thank Andrew Goertzen, Dr. Yiping Shao, and Dr. Indrin Chetty for sharing ideas concerning photon transport. We would also like to thank Dr. Simon Cherry, Dr. Arion Chatzioannou, and Dr. Freek Beekman for theoretical discussions and David McElroy, Larry Pang, and Ron Sumida for assistance with phantom scans. This work was funded in part by NCI grant R01-CA56655 and DoE Contract DEF G0387-ER6061.

VI. REFERENCES

[1] S.R. Cherry, S.R. Meikle, and E.J. Hoffman, "Correction and Characterization of Scattered Events in Three Dimensional PET Using Scanners with Retractable Septa", *Journal of Nuclear Medicine*, vol. 34, pp. 671, 1993

[2] J.M. Ollinger and G.C. Johns, "Model-based Scatter Correction for Fully 3D PET," *Physics in Medicine and Biology*, vol. 41, pp. 153-176, 1996

[3] I. Castiglioni, O. Cremonesi, M.C. Gilardi, V. Bettinardi, G. Rizzo, A. Savi, E. Bellotti, and F. Fazio, "Scatter correction techniques in 3D PET: a Monte Carlo evaluation," *IEEE Transactions on Nuclear Science*, vol.46, pp. 2053-2058, December 1999

[4] C.J. Thompson, J.M. Cantu, and Y. Piccard, "PETSIM: Monte Carlo program simulation of all sensitivity and resolution parameters of cylindrical positron imaging systems," *Physics in Medicine and Biology*, vol. 37, pp. 731-749, 1992

[5] M.S. Kaplan, R.L. Harrison, and S.D. Vannoy, "Coherent Scatter Implementation for SimSET," *IEEE Transactions on Nuclear Science*, vol.45, pp. 3064-3068, December 1998

[6] H. Zaidi, A. Scheurer, and C. Moral, "An object-oriented Monte Carlo simulator for 3D positron tomographs," *Computer Methods and Programs Biomedicine*, vol. 58, pp. 133-145, 1999

[7] Communication with I. Castiglioni, "The MC-PET Project: Building an open-to-public Database of Monte Carlo Data sets for PET," *Society of Nuclear Medicine Annual Meeting Program*, pp. 132, 2000

[8] H. Zaidi, "Relevance of accurate Monte Carlo modeling in nuclear medical imaging," *Medical Physics*, vol. 26, pp. 574-608, April 1999

[9] C.S. Levin, Y. Tai, M. Dahlbom, T.H. Farquhar, E.J. Hoffman, "Removal of the effect of Compton scattering in 3D whole body PET by Monte Carlo", *1995 Nuclear Science Symposium and Medical Imaging Conference Record*, vol. 2, pp. 1050-54, October 1995

[10] C.S. Levin, M. Dahlbom, and E.J. Hoffman, "A Monte Carlo correction for the effect of Compton scattering in 3D PET brain imaging," *IEEE Transactions on Nuclear Science*, vol. 42, pp. 1181-85, August 1995

[11] C.H. Holdsworth, "Investigation of Accelerated Monte Carlo Techniques of PET Simulation and 3D PET Scatter Correction," *IEEE Transactions on Nuclear Science*, December 2000

[12] C.C. Watson et al, "Evaluation of simulation-based scatter correction of 3D Cardiac Imaging," *IEEE Transactions on Nuclear Science*, vol. 44, pp. 90-97, February 1997

[13] E.R. Woodcock et al, "Techniques Used in the GEM Code for Monte Carlo Neutronics Calculation", *Proceeding on the Conference for Applications of Computing Methods to Reactors*, ANL-7050, pp. 557, 1965

[14] C.C. Watson, "A Technique for Measuring the Energy Response of a PET Tomograph Using a Compact Scattering Source," *IEEE Transactions on Nuclear Science*, vol. 44, pp. 2500-2508, December 1997

[15] D.R. Haynor, R.L.Harrison, et. al, "Improving the Efficiency of Emission Tomography Simulations Using Variance Reduction Techniques," *IEEE Transactions on Nuclear Science*, vol. 37, pp. 749-753, April 1990

[16] F.J. Beekman, E.T.P. Slijpen, and W.J. Niessen, "Selection of Task-Dependent Diffusion Filters for the Post-Processing of SPECT Images," *Physics in Medicine and Biology*, vol. 43, pp. 1713-1730, 1998

[17] K. Kitamura, H. Iida, M. Shidahara, S. Miura, and I. Kanno, "Noise Reduction in PET Attenuation Correction Using Non-linear Gaussian Filters," *1999 Nuclear Science Symposium and Medical Imaging Conference Record*, October 1999

[18] C. Riddell, P. Brigger, R.E. Carson, and S.L. Bacharach, "The watershed algorithm: a method to segment noisy PET transmission images," *IEEE Transactions on Nuclear Science*, vol. 46, pp. 713-719, June 1999

Send Correspondence To:

Clay Holdsworth
choldsworth@mednet.ucla.edu